



Spacecraft Scale Magnetospheric Protection from Galactic Cosmic Radiation

John Slough

EasyChair preprints are intended for rapid dissemination of research results and are integrated with the rest of EasyChair.

June 1, 2023

Spacecraft Scale Magnetospheric Protection from Galactic Cosmic Radiation

John Slough¹

MSNW LLC, Bellevue, Washington, 98008-5858

An optimal magnetic shielding configuration for significantly reducing astronaut exposure to Galactic Cosmic Radiation (GCR) on long interplanetary missions has been realized, and is referred to as the Magnetospheric Dipolar Toroidal Magnetosphere (DTM). This configuration was shown to have the singular ability to deflect the vast majority of the GCR including High Z Energetic (HZE) ions. This external (to the spacecraft) dipolar field is created by an array of unidirectional toroidal High Temperature Superconductor (HTSC) windings mounted externally on the surface of the toroidally-shaped spacecraft habitat. In this way the spacecraft directly supports the magnetic hoop forces generated by the toroidal currents and thereby significantly reduces the structural mass requirements for the shield. The magnitude of the toroidal currents are arranged poloidally to flow so as to maintain the spacecraft shell as a constant flux boundary where the magnetic flux is zero thereby keeping the spacecraft habitat field-free. As the dipole magnetic field is perpendicular to the spacecraft habitat in all directions, the DTM provides a deflecting shield to all the incoming GCR which is nearly isotropic. In addition, the DTM shields the HTSC magnets as well thus eliminating the secondary particle irradiation hazard, which can dominate over the primary GCR for shields with closed magnetic topologies. With DTM shielding it was found that both the structural and magnet mass as well as power requirements were significantly reduced. A 3-D relativistic particle code was used to evaluate shielding effectiveness for the GCR spectrum encountered in space. Four topics that will be covered involve a direct comparison of the three principal efforts developed to date for shielding; They are: (1) Effectiveness of the magnetic shielding (2) Issues with secondaries; (3) Launch and space assembly, and (4) Advantages and other uses.

I. Introduction

IT is well known that exposure to the ionizing radiation of galactic cosmic-rays (GCR) and solar energetic particles (SEP) is an important concern for the health of the crew for long duration interplanetary missions.¹⁻⁶ The question to be addressed here is whether or not it is feasible to mitigate this exposure in a practical manner. The GCR flux is near isotropic and is relatively constant, being modulated somewhat by the solar cycle. Periods of maximum solar activity result in the decrease of the low energy GCR flux due to their interaction with the higher particle flux emitted by the Sun. Previous analyses have pointed out the futility of attempting to employ a material barrier for the GCR as the increase in shield thickness creates a mass penalty that is far too great to be practical. Even partial shielding is not an effective option as the radiation hazard can actually be greatly enhanced in this case due to the “daughter” particles generated during the slowing down process of the GCR in the material. This is particularly true for the high charge and energy (HZE) ions such as iron which can create several

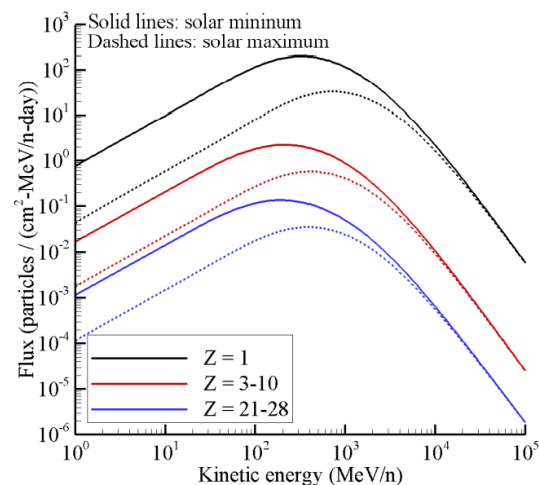


Figure 1. GCR flux at solar minimum and solar maximum. Z is the atomic mass of the GCR particle. (From Ref. 2)

¹ Director of Research, MSNW LLC, sloughj@msnwillc.com.

high energy secondary and tertiary particles. The radiation risk arises from the damage caused by the energy lost from these charged particles in human tissue. The GCR fluxes represent a longer-term risk exposing the crew members to lower life expectancy due to radiation induced cancers.

II. Analysis of Active Magnetic Shielding

Of all the active methods that have been suggested to take the place of passive (i.e. material) shielding, the most promising from a technological point of view, and the most studied, is the use of magnetic fields to deflect the GCR away from the human space habitat. The basis for this approach is given by the partial shielding provided by the Earth's magnetic field, however it is not Earth's magnetic field but rather the bulk of the Earth's atmosphere that protects us from the full brunt of the GCR. The physics behind the concept is simple and is based on the fact that a charged particle in traversing a transverse magnetic field will experience a transverse acceleration to its direction of motion due to the Lorentz force:

$$\vec{F} = q \vec{v} \times \vec{B} \quad (1)$$

As this is a non-central force, the kinetic energy of the particle is undiminished and is not reduced by this interaction. Only the direction of motion can be changed. In a uniform, transverse (to the particle motion) magnetic field \mathbf{B} the particle executes a circular motion at a radius r_L (Larmor radius) given by:

$$r_L = \frac{mv_{\perp}}{qB} \cong \frac{mc}{qB} \quad (2)$$

where it is recognized that these high energy (\sim GeV/nucleon) particles will be moving close to the speed of light so that m represents the relativistic particle mass. In order for a magnetic field to deflect a charged particle in a variable magnetic field, such as occurs in a magnetospheric dipole field, the integral of the magnetic field over the path of the particle motion within the magnetic shield must be sufficiently large (i.e. comparable to the gyro-radius of the particle) or,

$$v_{\perp} \cong \frac{q}{m} \int B_{\perp} dr \quad (3)$$

where q is the charge of the particle, and the subscript \perp denotes quantities perpendicular to the magnetic field. Any particle with v_{\perp} less than the value found from Eq. (3) will be deflected, irrespective of its initial pitch angle. For shielding of MeV protons and 1 GeV electrons, Eq. (3) then requires that $\int B_{\perp} dr$ be of the order of 0.1 Tesla-meter (T-m). Deflection of a GeV proton would then require $\int B_{\perp} dr$ to be of the order of 3 T-m while solar wind particles would only require 0.001 T-m. This criterion is a necessary condition but it turns out to not be a sufficient condition. Magnetic shielding must be verified by single particle tracking techniques like those that were developed in this study, and similar to the Monte Carlo techniques developed elsewhere for this purpose.⁷⁻⁸

For scaling purposes though the simple deflection picture is adequate. In a spatially uniform magnetic field, the distance L the particle must travel transverse to this B field to be deflected by an angle θ is given roughly by:

$$\theta = 2 \sin^{-1} \left(\frac{2L}{r_L} \right) = 2 \sin^{-1} \left(\frac{2}{c} \frac{q}{m} BL \right). \quad (4)$$

Clearly one wishes to maximize B and L . The other key variable is the charge to mass ratio q/m . This is where active magnetic deflection has a great advantage over passive shielding. This ratio is roughly constant at ~ 0.5 coulomb/nucleon as one goes from helium to iron. While hydrogen has a somewhat more favorable ratio (unity), the magnetic field deflection of HZE ions like iron will be as effective as that for deflecting lighter ions with the same charge to mass ratio. This of course is with the caveat that these HZE ions do not encounter material objects. In that case the tissue damage from the subsequent particle cascade can more than make up for their much lower GCR population.

III. Past Efforts on Active Magnetic Shielding

There have been several groups that have presented active shield designs based on superconducting magnet configurations. Virtually all have assumed shield configurations composed of toroidal or solenoidal magnets. There is a very good reason for this. With the advent of High-Temperature Superconductors (HTSC), it is possible to achieve very high magnetic flux densities at operating temperatures (~ 25 - 75 °K) that do not require the use of liquid helium thereby alleviating the technical difficulties in providing for the stability of a cryogenic system in space. There have

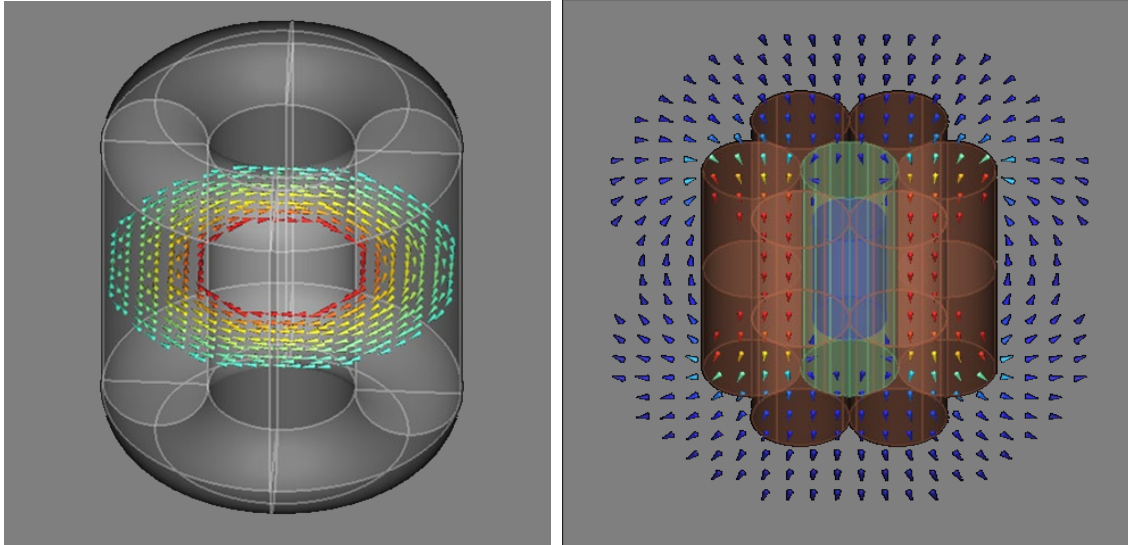


Figure 2. 2D magnetic vector plots for (Left) ESA toroid at midplane, and (Right) 6-1 Solenoids. *The vectors are color coded red to blue indicating magnitude of the field. The plots range from the maximum field down to 5% of the maximum. The ESA toroid had no external fields larger than 1% of the maximum outside of the torus.*

been two main studies employing HTSC shields that employ B field coils partially surrounding the spacecraft habitat with the high magnetic fields concentrated in a layer radially outward from the habitat (see Fig. 2). These were performed by the European Space Agency which employed a toroidal magnetic geometry (ESA toroid)⁹, and The NASA NIAC study⁴ which employed a circular array of 6 large solenoidal coils with a central seventh coil operated in the reverse sense to buck out the magnetic field created by the six surrounding solenoids (NASA 6-1 Solenoids).

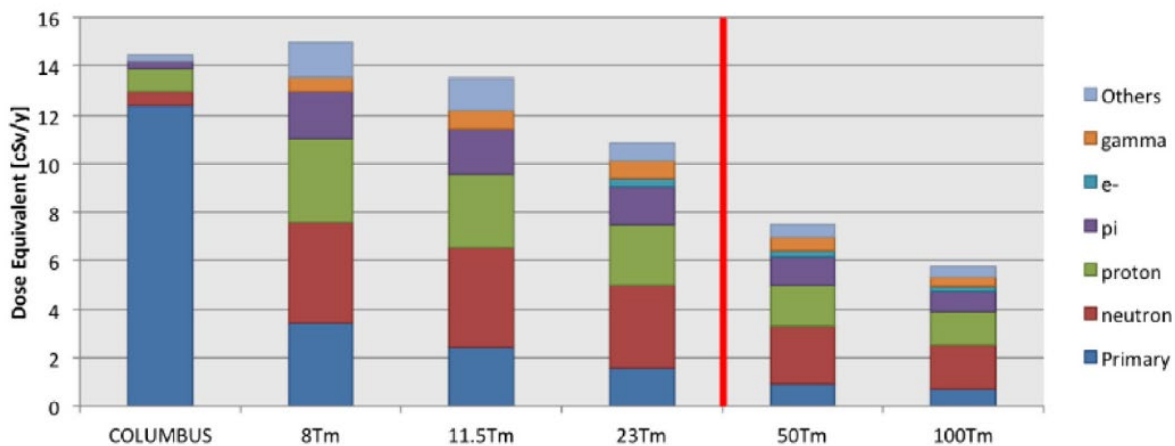


Figure 3. The annual body dose equivalent of the primary GCR proton and He nuclei, with a breakdown of the contribution of each of the principal secondary particles. *The 50 and 100 T-m configurations require field flux densities that exceed the performance of present-day HTSC. (From Ref. 1)*

The idea being in both cases that a high B·L product can be achieved at least for GCR flux coming in the radial direction toward the habitat.

The HTSC shields for the studies were as follows: Yttrium-Barium-Copper-Oxide (YBCO) for the NASA 6-1 Solenoids and Magnesium Diboride (MgB_2) for the ESA Toroid. The performance of these designs was evaluated based on the results obtained with 3-dimensional Monte Carlo simulations that propagate the charged particles in the magnet field, and generate interactions of the particles in the materials of the coils and support structures of the magnet shield. Even with extrapolations of existing technology for the materials of the coils and support structures of the magnet shield, the results were not encouraging. The results from the calculation can be found in Fig. 3 taken from Ref. 1. The performance is expressed in terms of the contribution of the field to the overall dose reduction of the shield, including the passive shielding elements, and the combined shield plus habitat dose level with respect to the habitat dose level with no shield. Neither the ESA Toroid or the NIAC 6 - 1 Solenoids have any significant magnetic field on the spaceward side of the coils, these systems are completely vulnerable to all GSR, even the lowest energy ones that would be deflected by the shield. They strike the both magnets and supports structures which are much larger than the habitat they're trying to protect. This interaction with these elements lead to the creation of daughter particles. As can be seen in Fig. 3, the role that the magnetic field plays in reducing the primary GCR is significant but the total effect on radiation exposure is paltry at best. The NASA 6-1 Solenoids numbers are close to having no net effect at all. It should be noted that the GCR that come from the polar regions (see Fig. 2) were not considered, so even the magnetic shielding reduction in Fig. 3 is an overestimate as it does not reflect these marginally deflected particles.

This additional lack of efficacy stems from the magnetic topology of the approaches taken in these concepts. It is clear from Eq. (3) that to deflect the GCR particle, the magnetic field must be perpendicular to the direction of motion. Since particles can come from any direction, deflecting only those coming in perpendicular to the primarily axial or azimuthal B field will not suffice. This “hole” on-axis allows primary GCR to enter unabated. In fact, some GCR particles can be deflected into this region by the very fields meant to keep them out. The results from the GCR particle tracing to be discussed later clearly illustrate this vulnerability, particularly for the ESA toroid.

IV. Dipolar Toroidal Magnetosphere (DTM) Shielding

It can be readily argued for active magnetic shielding to be a viable option, that at a minimum the following criteria must be met: (1) The magnetic shield must deflect the vast majority of GCR ions including HZE ions. (2) The magnets must not create additional high energy particles from passive absorption. (3) The structural, mass, and power

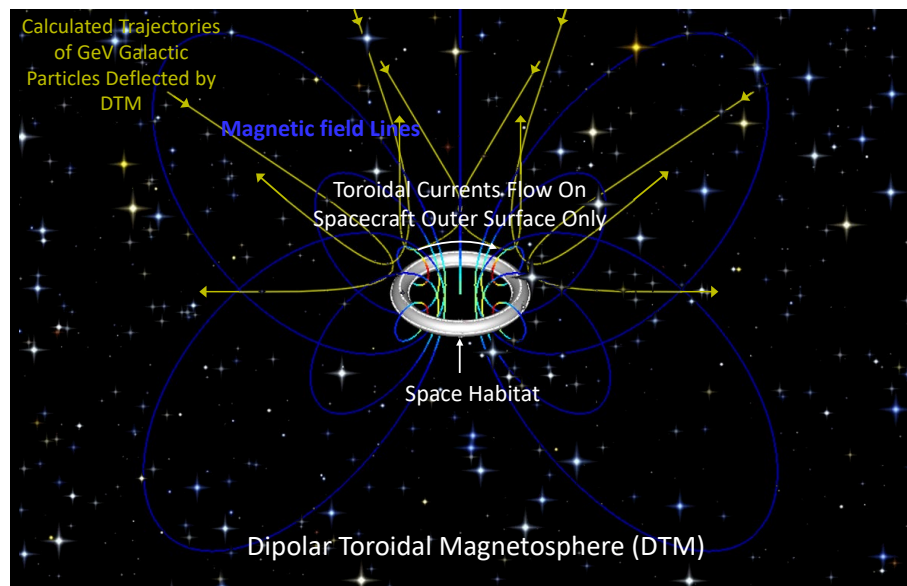


Figure 4. Dipolar magnetospheric shielding provided by toroidal currents I_c . The HTSC magnet (silver colored shell) is placed external to the toroidally shaped space habitat. The magnet would fully surround the habitat to assure cancellation of all magnetic field inside the habitat.

requirements for the shield must not become “the tail that wags the dog”. (4) The shield development roadmap must allow for both analytical and experimental validation at much reduced cost and scale prior to full deployment.

It is believed that all four of these criteria can be met by the shielding concept described in this section. It is also believed that the magnetospheric approach taken here is likely to be the only one that can. There are very good reasons for that belief based on the physics and topology requirements for an effective shield. To understand why previous conceptual designs have failed to satisfy these criteria, and how the proposed approach avoids these pitfalls, a brief discussion will be given that illustrate the key principles that must guide the design of an effective magnetic shield. Adequate shielding in all directions, as well as protection of the magnets themselves can be accomplished by employing a Dipolar Toroidal Magnetic (DTM) field, where the habitat takes on the form of the shielding magnets as depicted in Fig. 4. In this way the spacecraft can directly support the magnetic hoop forces generated by the toroidal currents and thereby significantly reduce the structural mass requirements for the shield. It should be noted that the dipole currents all flow around the toroid in a shell surrounding the habitat, but in the same *toroidal* direction. In the ESA studies the coils also have a toroidal geometry. In this case however, the currents flow only in the poloidal direction, as is typical for a conventional toroidal magnet, thereby creating a toroidal field only on the inside of the toroid. This region is thus inhabitable and the structures required to support the coils adds considerable additional

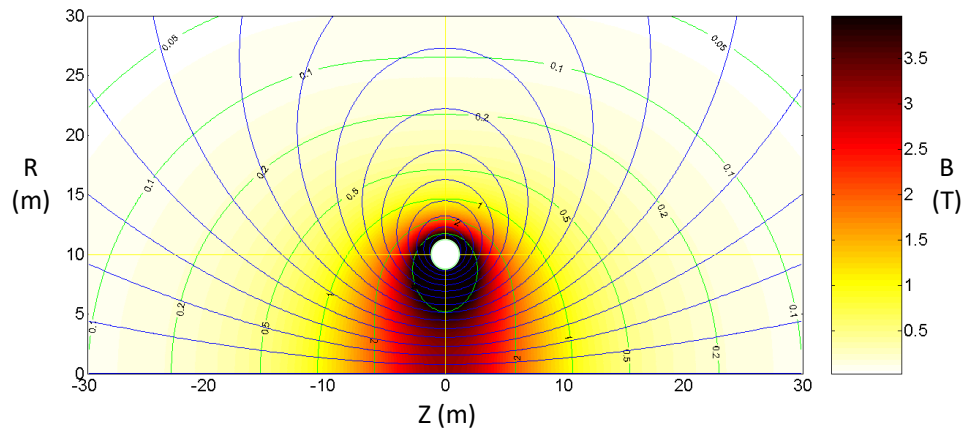


Figure 5. Flux lines and magnetic contours for a dipole torus. Here the current flows only at the toroid surface such that the magnetic field vanishingly small inside.

mass. This same shortcoming can be found in the NASA 6-1 Solenoids where an array of six, long solenoidal magnets surrounded the spacecraft and required an additional coil to buck out the return flux from these coils from the spacecraft habitat which diminishes the effective shielding. More will be said of these two concepts in the next section as they comprise the leading alternative magnetic shield concepts prior to this study.

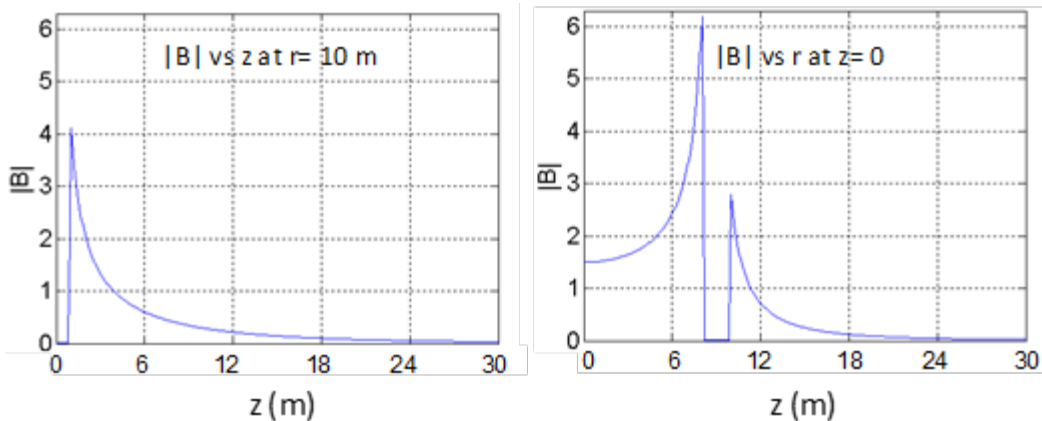


Figure 6. Modulus B as a function of z on axis and at the major torus radius R = 10.

In contrast, the external dipolar field created by the unidirectional toroidal currents in the shell all add to the strength of the external dipole field outside the space habitat. In this scenario, there is no need for providing additional

coils to cancel the internal fields as in the other approaches. The toroidal currents are arranged to flow so as to maintain the shell as a constant flux boundary where the poloidal flux $\phi = 0$. It is easiest to see how this can be arranged by considering a cylindrical tube carrying a uniform axial current along its length. The B field created is purely azimuthal (i.e. poloidal) and vanishes inside the wall of the cylindrical conductor, which can be easily confirmed by a simple application of Ampere's law at any radius inside the cylinder. Bend this cylindrical tube into a torus and you have the situation desired here. The toroidal currents in this case however do not flow at a constant magnitude at all azimuthal angles around shell periphery as it does for the cylinder. Only for torii at very large aspect ratio (torus diameter/habitat diameter $\equiv \alpha$) does it approach uniformity. For a typical aspect ratio $\alpha \sim 10$, a larger current must flow on the inner wall of the torus to maintain the $\phi = 0$ state inside the habitat (see Figs. 5 and 6).

Analysis of the shielding for this dipole torus was conducted with a particle tracing code developed at MSNW. The magnetic field and flux for a realistic scale dipole torus is shown in Fig. 5. The magnetic field strength is characterized by the magnetic field B_{00} at $r = z = 0$. Plots of the magnetic field on axis and at $r = 10$ m as a function of z is shown in Fig. 6 which clearly show how the field (and thus I_ϕ) is significantly higher on the inboard side of the torus for a toroid with an $\alpha \sim 10$ as is the case here. The characteristic axial field strength on axis at the center of the toroid, $B_{00} = 1.5$ T for this case. The effectiveness of the magnetospheric dipole in deflecting GeV GCR particles can be seen in Fig. 7 where it was found to be sufficient to exclude all particles from a significant volume about the dipole. This is clearly where one would place both the space habitat and toroidal coils providing full protection from GCR bombardment.

From both a confinement and shielding perspective, as well as the obvious choice for simplicity, shielding from an array of geometrically simple circular loops of conductors as proposed here was found to be the most favorable. A code to calculate the particle motion in a 3-D magnetic field was developed and tested, and was found to be quite accurate. It is possible however to do some analytic estimates that reproduce with reasonable accuracy the results from the 3-D numerical calculations. Since it is easy to calculate the field from a single loop (or sets of loops as in the toroidal shield), the shielding effectiveness can be characterized by the B_z field on axis at the center of the toroid (B_{00}), and the far-field dipole magnetic field $B_z(r)$,

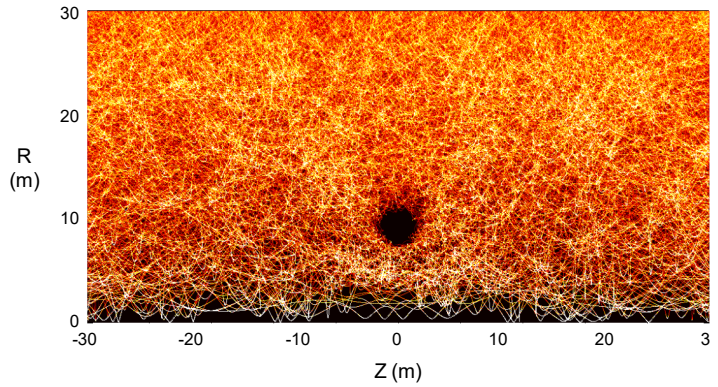


Figure 7. Trajectories of 1500 isotropic 1 GeV particles on to dipole ring. Apparent shielding at small r only reflects the volume reduction as $r \Rightarrow 0$.

$$B_{00} = \frac{\mu_0 I}{2R} \text{ and } B_z(r) = g B_{00} \frac{R^3}{r^3}, \quad (5)$$

where it was found that $g = 0.5$. B_{00} is typically less than the field strength at the torus boundary but serves the purpose of relating the field strength to the shielding effectiveness. If one assumes that an incoming particle penetration distance must be less than a characteristic deflection distance (see Eq. 4), one has

$$\int_{l_1}^{l_2} \frac{dl}{r_L} \geq 1 \rightarrow \int_{r_0}^{\infty} B \cdot dr \geq \frac{m}{q} \gamma v \quad (6)$$

where the relativistic nature of the GCR particle is explicitly expressed. Integrating using Eq. (5) one obtains:

$$B_{00} \geq \frac{m}{q} \frac{4\gamma v r_0^2}{R^3} \sim \frac{m}{q} \frac{4\gamma v}{R} \quad (7)$$

Where the approximation assumes that smallest characteristic deflection radius r_0 is assumed to be roughly that of the torus radius R . For a 1 GeV proton one has $\gamma v = 5.4 \times 10^8$ m/s. For a loop radius of 10 m one has $B_{00} \geq 2.2$ T. This turns out to be somewhat more restrictive than the detailed particle calculations, but close enough for most purposes such as scaling, current, and structural requirements. The results from the particle calculations for the Dipolar Toroidal Magnetosphere (DTM) with $\alpha = 10$ are shown in Fig. 7. It can be seen that complete shielding can be obtained for higher energy nucleons by increasing the magnetic field and that partial shielding is possible even at higher energies although the effectiveness diminishes for these higher energy GCR particles.

V. Comparison of prior proposed magnetic shielding geometries to the DTM

Several different magnetic configurations were evaluated taking into consideration both feasibility and simplicity. In order to make such a comparison it was necessary to develop criteria that would be critical, if not essential for the implementation of the concept as a feasible system for further development. Four criteria were arrived at and are stated below:

- (1) *Effectiveness of the magnetic shielding* – This will be determined using the Ω parameter to be discussed and defined in section A below as it is the best measure of the protection realized for a given habitat and magnetic geometry as a function of the magnet mass required.
- (2) *Issues with secondaries* - The interaction of the magnetic structural topology for each concept can have a significant effect on the type of radiation exposure experienced inside the habitat from the structures themselves regardless of the effectiveness of the magnetic deflection from the magnet.
- (3) *Launch and space assembly* – The amount of mass, scale of structures, and complexity of assembly of the magnet systems must be characterized as the cost of access to space is still a determining factor in concept feasibility.
- (4) *Advantages and other uses for the shield outside GCR protection*. Given the likely high cost of the shielding systems, what other uses for the shield might there be besides crew protection that would help justify the investment in the shield deployment.

These four criteria, and how they measure up for the three most developed and promising concepts, will now be discussed.

A. Effectiveness of the Magnetic Shielding

This is clearly by far the most significant. For “open” systems where the magnetic field is not primarily confined by a conducting boundary, the best candidate is the magnetic dipole as it has the slowest falloff with distance ($B \sim 1/r^3$). For a closed magnetic geometry, there appear to be two well researched and characterized candidates, the NASA 6-1 Solenoids and the ESA toroid discussed earlier. These two will now be characterized, along with the DTM, using a commercial 3D code from Integrated Engineering, Lorentz-3M[®], that can accurately calculate the magnetic fields from any specified array of current elements, as well as track the relativistic trajectory of emitted particles in these fields. By using this code, an unbiased and accurate comparison of the relative effectiveness of the proposed shield concepts was made.

Just as important as the calculation accuracy is a method for normalizing the results across all three concepts, so that a valid comparison can be made as the total current requirements, magnetic field strengths, and magnet mass are all different for each model. It is contended here that the normalization criteria should be the total HTSC mass required for a given GCR reduction normalized to the habitat volume, V_{hab} . The additional mass required in space to protect a given spacecraft habitable volume is clearly a major factor. As different concepts considered different types of High Temperature Superconductor (HTSC), and at different current densities, a better metric is the total of the currents required, I_{tot} times each conductor length, L_c , required. This quantity is independent of the type of HTSC and assumed maximum current density J_{cr} . It is however directly proportional to magnet mass. Once the optimal HTSC and its maximum current density has been determined, it should be the same for all concepts. This key ratio: $I_{tot} \cdot L_c / V_{hab} \equiv \Omega$, is thus the primary criterium in evaluation of the effectiveness of shield. The characterization of the shielding concepts represented by the ESA toroid, the NIAC 6-1 Solenoids, along with the DTM will now be described in more detail. These formed the basis for the input into the Lorentz 3M calculation carried out identically on all three concepts.

Figure 8 illustrates the setup for the magnetic coil (current) surfaces and habitat assumed by the various concepts inside a semitransparent sphere which defined the launch surface for the GCR particles, and formed the basis for the input into the Lorentz 3M calculation carried out identically on all three concepts. As was mentioned the analysis of the efficacy is measured by the total HTSC mass per unit volume of habitat, or

$$\Omega = \frac{\sum_1^n I_n \cdot L_n}{Vol_{Hab}} \quad (8)$$

where the sum is over all the current elements times the length of that current element, and Vol_{Hab} is the total volume of spacecraft habitat protected by the magnetic shield. In previous studies the assumed HTSC and maximum current density was folded in to both the mass calculation as well as the size of the field generated, which made comparisons difficult. Here it is assumed that the optimal HTSC for shielding should be independent of the magnetic system employed, and avoids a down-select until the optimal configuration has been determined based on Ω . It should be noted that the habitat size, shape and volume are not independent variables. Variations in scale for a given topology will reflect different Ω 's. Generally speaking, the larger the habitat, the less Ω is required. There is no easy way to normalize the habitat for all three concepts, and using the actual habitat geometry and size proposed was the next best option. Doing so allowed for the extensive Geant 4 radiation calculations¹ performed on these concepts to be used in helping to assess issues in regards to secondaries (see criteria 2 above).

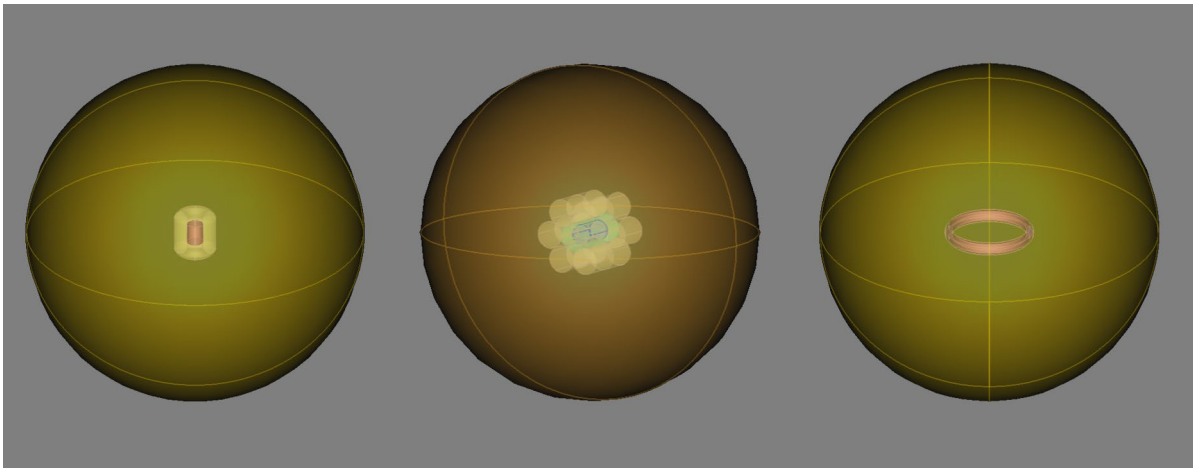


Figure 8. Spherical surfaces for the random launch of GCR test particles for isotropic bombardment of the three magnetic shield configurations. *The magnetic coils are shown as semi-transparent with the habitat incased within as described for the three concepts. The meridian lines are for showing position of spherical surface and had no significance with regard to the calculations.*

There was also no reason to use the entire GCR spectrum in evaluating the three concepts as the principle means of protection (magnetic deflection) is more easily observed under simpler, but an equally accurate assumption for comparison purposes. Given the seasonal variation in GCR exposure as well as the essentially untested dependence of radiation risk on GCR energy, it was decided not to fold these considerations into the comparison. That is not to say these considerations are not important, but again it is something to consider after choosing the best magnetic shield configuration in deflecting any GCR. It was thus decided to carry out the comparison for deflection of the GCR at the peak of the GCR radiation power curve, and for the largest contributor at that energy. In other words, an isotropic emittance of 500 MeV protons was used to test the three concepts.

The 500 MeV protons were launched from the surface of a sphere with a 100 m diameter for all three cases. The large standoff was necessitated as the GCR deflection from the DTM's external field was still significant at large distances from the toroidal dipole coils. The difference in deflection effectiveness was becoming small enough at a launch radius of 50 m that it made only slight differences (< 5%) compared to 100 m. The smaller launch radius of 50 m was still much greater than used in previous calculations for the ESA and NASA concepts. The GCR source sphere in relation to the three coil systems and habitats can be found in Fig. 8. Over twenty thousand protons were launched at random angles. The angular spread was governed by a cosine distribution to the normal at any given point on the sphere to avoid launches far from the target direction in order to keep the calculation time reasonable. With the magnetic field turned off, roughly two thousand, 500 MeV protons struck and were collected on the habitat surfaces.

The total current in the coils was then increased until at least 75% of these protons were deflected so that they failed to reach the habitat surface and were terminated back on the spherical launch boundary (see Fig. 9).

The measured shielding efficiency, Ω , between the concepts was dramatic. The Ω value for the three cases at 75% primary proton deflection was: $\Omega = 55 \text{ MA-m}^{-2}$ (ESA Toroid) = 22 MA-m^{-2} (6-1 Solenoids) = 1.7 MA-m^{-2} (DTM). The DTM was found to be over an order of magnitude better at shielding per unit habitat volume than the other two concepts. Plots of the fraction of the primary 500 MeV protons that were collected at the habitat surface, f_{col} , as a function of total current can be found in Fig. 9. There are several reasons for this. The toroidal current loop for the DTM is large and while it is the product of the current times the loop length that determines the magnet mass, the much larger scale of the magnetic field generated more than makes up for this. For the ESA toroid case, there are two reasons that the results were more unfavorable for this magnetic configuration. The biggest problem was the lack of protection for GCR that can enter through the end regions at the toroid hole. The toroid is a good deflector of GCR coming in more or less radially from what was referred to as the “barrel region”. After a precipitous drop in penetration from these protons the level of protection plateaus around 40 % of the unshielded case, and increases in coil current have only a marginal effect. This is simply due to essentially no magnetic protection over a wide solid angle at each end. The magnetic field is contained only inside the toroid which leaves these regions completely exposed. The axial entry is also an issue for the 6-1 solenoid. The primary deflection is only for GCR particles that enter the coils in the direction perpendicular to the axis of the coil magnetic fields. The NASA 6-1 Solenoids case is not as bad as the ESA toroid because the solenoids are essentially very elongated dipoles and the return flux from the coils’ interior region is not cancelled by the reverse coil so that there is some external field protection in the end region from the return flux (see Fig. 2). The answer as to criterium (1) then is that the DTM is considerably more efficient in providing GCR shielding, and has the capability to completely extinguish GCR up to an energy determined only by the strength of the magnetic field.

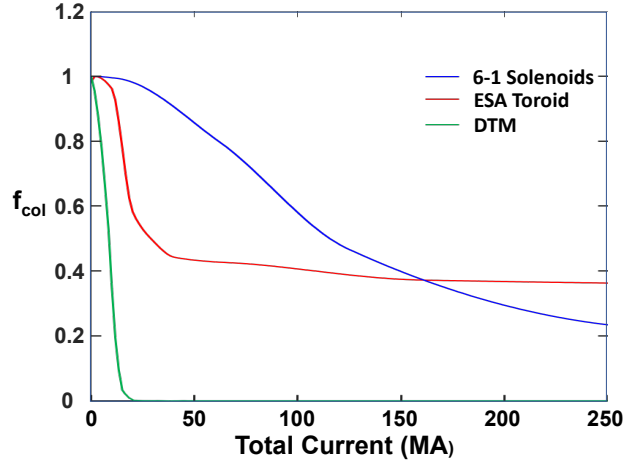


Figure 9. Fraction of 500 MeV protons reaching the habitat of the various concepts as a function of the total current.

B. Issues with Secondaries

A critical consideration is whether the magnet system itself poses additional radiation concerns due to daughter particle generation from GCR striking the large magnet structures. As mentioned, previous analysis of the “closed-field” concepts indicate that this turns out to be a very significant problem for as there is very little, if any, deflection of GCR external to the magnet. With the coils placed in a manner that engulfs the habitat along with the fact that the extent of the coils being considerably larger than the habitat itself, creates a much larger source for this particle-cascading process and it occurs prior to any significant reduction in GCR flux. Clearly, by deflecting the vast majority of GCR prior to reaching the magnets and/or habitat as is the case for the DTM, the problem of secondaries is considerably mitigated. While one anticipates that there will be no secondary issue for the DTM, it is made even more assured with the employment of discrete cables of HTSC current carriers as will be seen in section VI. It is left to future work to apply the Geant 4 code and provide a definitive measure of the reduction from secondary particle exposure

C. Launch and Space Assembly Issues

There are several other elements that could favor one approach over another such as the ease of assembly of the structures and coils required in space. The ability to launch subassemblies for easy assembly is clearly a plus. Another important element is the maximum magnetic field stress felt by the magnet structural system. This is harder to normalize due to the different habitat configuration geometries. It should however be a part of the criteria in a general way as the structural magnet mass requirement will be driven by the maximum surface area, A_s , exposed to the magnetic field as the force on the structure scales as $B_s^2 \cdot A_s$. All three of the concepts described in section III will

require some form of space assembly, however the much larger magnetic coils and fields for the ESA toroid and NIAC solenoids put them at a greater disadvantage here. With the reduction in field required for the DTM, along with the likelihood that the supporting framework for the HTSC coils can be integrated into the spacecraft external wall structure, it should be possible to deploy the DTM without a significant mass penalty. This needs however to be more critically evaluated.

D. Advantages Beyond GCR Protection

Finally, can the magnetic deflection scheme employed for optimal shielding effectiveness (e.g. the toroidal geometry of the DTM) provide for additional benefits in terms of human health? With a large aspect ratio toroidal habitat, the possibility of an artificial gravity can be readily achieved through simple rotation of the torus in the toroidal direction. Evidence from spaceflight and spaceflight analogs such as the NASA Human Research Exploration Analog (HERA) suggests that the Risk of Adverse Cognitive and Behavioral Conditions and Psychiatric Disorders (BMed) poses a high probability and high consequence risk for extended and planetary exploration⁹. Given the possible synergistic effects of prolonged isolation and confinement, radiation exposure, and prolonged weightlessness, mitigating such enhanced risks faced by future crews are of highest priority. It is likely that isolation and confinement can only be resolved by shorter trip times¹⁰. The radiation exposure and prolonged weightless can be simultaneously resolved by implementation of the DTM.

VI. Evaluation of the DTM Shielding Effectiveness Across the GCR Spectrum

Given that the DTM can perform reasonably well for all four criteria, it is worth a more detailed evaluation of its performance across the GCR spectrum. The protection observed needs to be stated in terms of a set of independent variables that characterize the deflection as a function of particle energy, charge to mass ratio of the GCR, and the radius and characteristic magnetic field strength of the DTM in the plane of the DTM at the axis of symmetry (B_{00}). The GCR have typically relativistic energies, so this must be taken into account as well. Recall that the condition for complete deflection of the GCR for the DTM one has:

$$B_{00} = C_B \frac{m_0}{qR} \gamma \beta c, \quad (9)$$

where C_B is a constant depending on toroid geometry, R is the major radius of the toroid, m_0 is the GCR particle rest mass, and q its charge. $\beta = v_{\perp}/c$. It is useful to write the relation for γ and β as:

$$\gamma = \frac{E_{tot}}{m_0 c^2} = \frac{E_k + E_0}{m_0 c^2} = \frac{E_k}{m_0 c^2} + 1, \quad (10)$$

$$\beta = \sqrt{1 - \frac{1}{\gamma^2}} \quad (11)$$

where E_{tot} is the total particle energy, and E_k is the kinetic component that is commonly used to characterize the GCR particle, and typically in units of GeV ($1 \text{ GeV} = 1.602 \times 10^{-10} \text{ Joules}$).

It was found that for a toroid similar to that used in the comparison study, but with discrete current elements instead of a toroidal current sheet, the effectiveness of the bundled currents actually improved the shielding effectiveness. The magnitude of the magnetic field where shielding starts to become less than complete was decreased by roughly a factor of two so that one has $C_B \sim 1$ in Eq. 9. As also seen before in the initial particle trajectory calculations, the attenuating effect of the dipole fields extend to larger energies, not vanishing until the particle energy is over a factor of two larger than the threshold value indicated in Eq. (9). In order to evaluate the effect of the DTM on GCR it is useful to recast the usual way the GCR flux is plotted i.e., as a log-log plot over a spectacularly large range of fluxes and particle kinetic energies (e.g., see Fig. 1). It should be noted that the particle flux drops precipitously from its peak around $\sim 300 \text{ MeV}$. As the relevant scaling parameters for the relativistic GCR are those of Eq. (9), and using Eqs. (10) and (11), the abscissa can be stated as simply $\gamma \beta$, where it is recognized that the rest energy of a nucleon (proton or neutron) is, $E_k^{nuc} = m_0 c^2 \cong 0.94 \text{ GeV}$. From Eqs. (10) and (11) one can see that for large gamma the relationship

between E_k and $\gamma\beta$ is linear. However, in the range of the highest flux of GCR (0.05 to 2 GeV) it is not. As an aid for conversion from the usual MeV/nucleon abscissa, a plot of E_k as a function of $\gamma\beta$ is found in Fig. 10

It is now possible to calculate the effect on the GCR spectrum for a 10 m radius torus with an aspect ratio of 7 carrying sufficient current to provide a $B_{00} = 0.64$ T, which for Hydrogen using Eq. (9) with $C_B \sim 1$, corresponds to a value of $\gamma\beta = 2$ for the full deflection of Hydrogen GCR with values of $\gamma\beta$ equal to and less than 2 (or equivalently ≤ 1.2 GeV). The attenuation of the GCR then tapers off over the first octave of higher energies to eventually no attenuation.

The plots for the principal bad actors: Hydrogen, Carbon, and Iron are shown in Fig. 11. One can see that for a fairly modest magnetic field, the shielding of GCR can be quite effective with the DTM. If one increases $B_{00} = 1$ T the results are even more notable as this extends the attenuation to the point where the natural falloff in flux reaches a low enough level that the remaining GCR that get through is negligible. As can be seen in Fig. 11, the mass to charge ratio for elements other than Hydrogen is twice that of hydrogen so that the effect of the shielding is diminished by a factor of 2 for the same B_{00} .

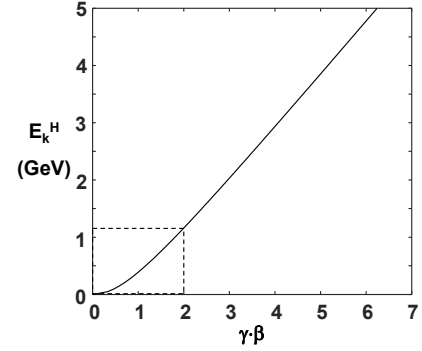


Figure 10. Relativistic proton energy as a function $\gamma\beta$.

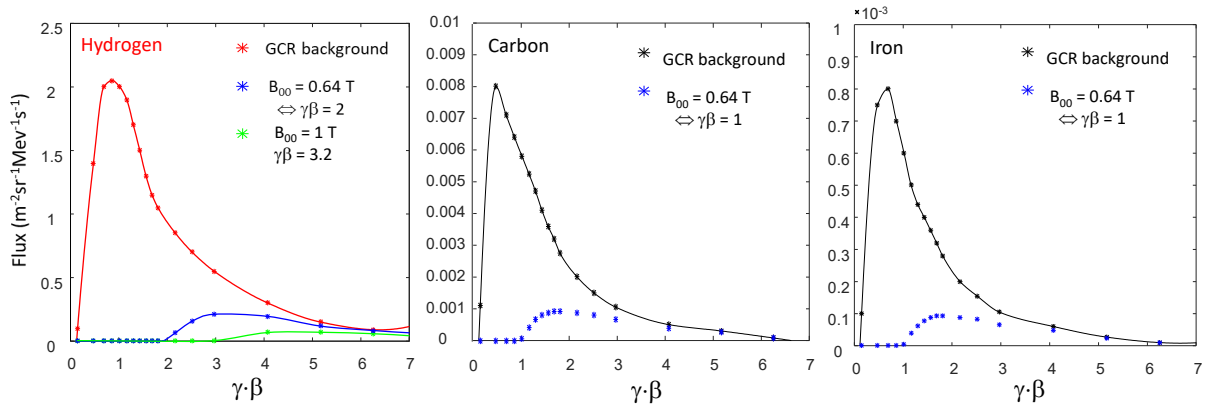


Figure 11. Predicted attenuation of the GCR spectrum from a Dipolar Toroidal Magnetosphere (DTM) where the toroid radius is 10 m and the aspect ratio = 7.0.

It should be noted that the protection indicated by these results are roughly a factor of two better than the calculations discussed earlier. At first it was thought that the improvement could be due to the small changes in aspect ratio of the habitat shape in going from circular to elliptical. Further calculations showed that these changes made only small differences. It should be recalled that all of the concept comparison was performed with uniform and continuous sheet currents. This was done primarily due to the fact that both the ESA toroid and the 6-1 Solenoids had assumed this current distribution in their shielding analyses. For the DTM, however, it was found that concentrating the current in bands of current carriers (20 in all) separated by gaps of slightly larger extent was considerably more favorable. It was thought that this would aid in protecting the coils themselves as well as provide port access in the habitat for space observation, solar power input, communications, etc. It turns out that this was a fortuitous choice as will now be discussed

The desire here was to evaluate the local behavior of the GCR near the HTSC coils. The 3D Monte Carlo codes employed in previous efforts elsewhere⁷ were not an option as they would not be adequate to resolve the particle motion to the accuracy desired in the near field of the coils as the GCR approach the current conductors. There is one very important advantage that came from the original numerical work performed with the MSNW code in that the resolution could be enhanced in such a way so that details of the particle's trajectory within the magnets could be analyzed. It was clear from the analyses by other groups employing the Geant 3 and 4 codes^{1,8} that the interception of the GCR by various structures can be quite deleterious as attested by Fig. 3. For the DTM, the largest deflecting magnetic fields are just *outside* the conductors and should therefore offer significant protection for the coils themselves. As this effect concerns the very local behavior of the GCR particle in the near field of the coils, the code

was modified to analyze this effect. This added protection in fact was borne out by the high-resolution trajectory calculations where the initial GeV nucleons were directed at the coils, and where the strength of the magnetic field was reduced to be insufficient to deflect the particles completely away from the habitat (see Fig.12). While there is little concern with damage to the coils from the GCR as the energy flux is miniscule, it would be advantageous to keep the magnet currents in bundles or cables as this will minimize daughter particles from being generated from collisions of the highest energy GCR with the coils.

As Fig. 12 clearly shows, the protection of the coils is enhanced by local current concentrations rather than a uniform distribution. What wasn't immediately obvious was whether this bundling and would provide for a more effective shield for the same total current. The Lorentz 3D code calculations for the DTM described earlier were repeated but this time with twenty cablelike bands as current carriers. This was done with an overall transparency of 50%. The cross-sectional volumes were proportional to the current required at that poloidal position to null the field inside the habitat. The total sum of all 20 currents was kept the same as the total surface current used in Section III for the comparison. The result was roughly a factor of two improvement in the shielding effectiveness, which was now in line with what was observed in the experiments.

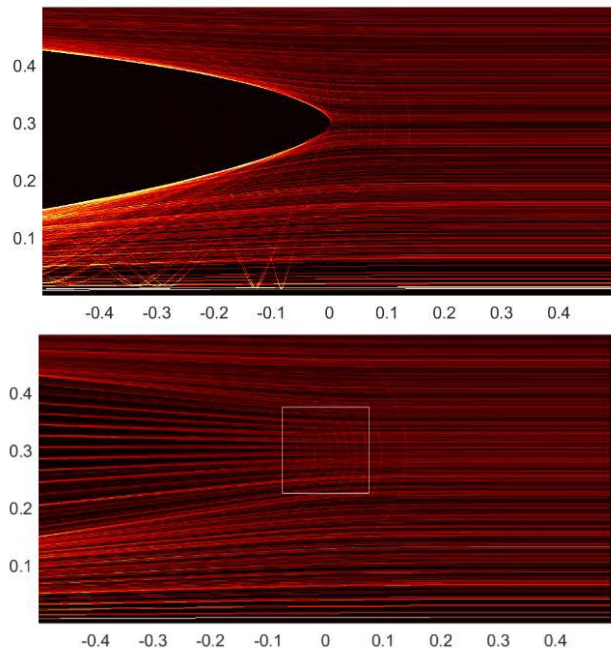


Figure 12. The figures above showing the difference in particle trajectory for a single, large current (top) as compared with a 15×15 current grid located inside square with the same total current (bottom).

VII. Application of the DTM Concept to the NASA Mars Habitat Module

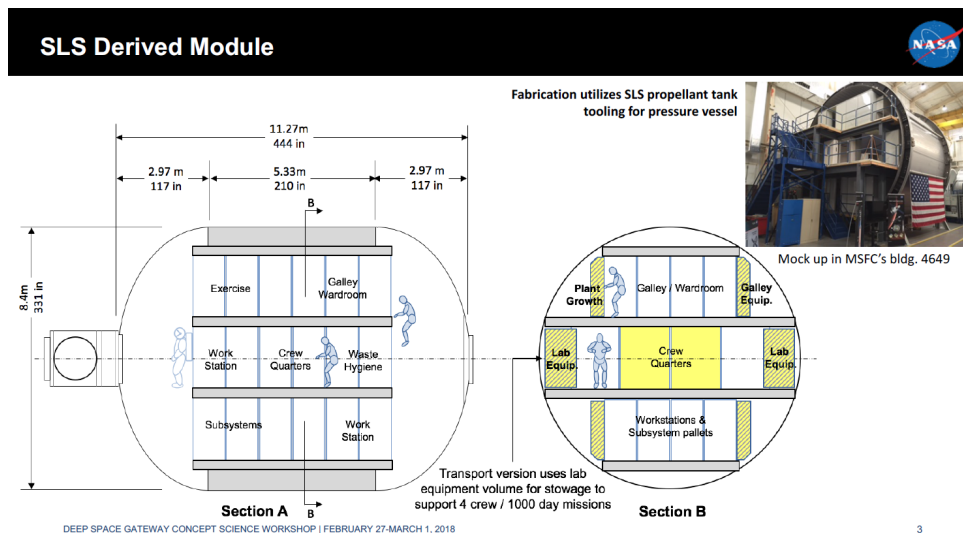


Figure 13. Proposed habitat and scientific laboratory for deep space missions.

It is clear that adopting the DTM that has been analyzed up to this point as a Deep Space Habitat (DSH) would require a significantly different space habitat than anything that NASA has considered in the past. Given that the DTM is a feasible, cost-effective, and more advantageous approach to GCR protection for humans, in addition to the fact there

is no other reasonable paths at this point, one must consider whether it is worth a change in scope to include a DTM to protect humans from GCR. Something that could possibly be more important for the health and well-being of the astronauts is the fact that the DTM would provide for a simple way to create an artificial gravity. Given that the much less-challenging plans that have been developed, such as those associated with DRA5, it is worth examining what one might be able to do with magnetic field protection given the constraints of the typical designs that have been already generated. Such an effort was undertaken using the SLS Derived Module which was part of the Deep Space Gateway design study. A graphic summary of this module is shown in Fig. 13.

It is worth noting that the performance of the magnetic field shielding found in the comparison study of section III, there is the possibility of employing a toroidal coil set for the generation of a closed field topology (it is noted that

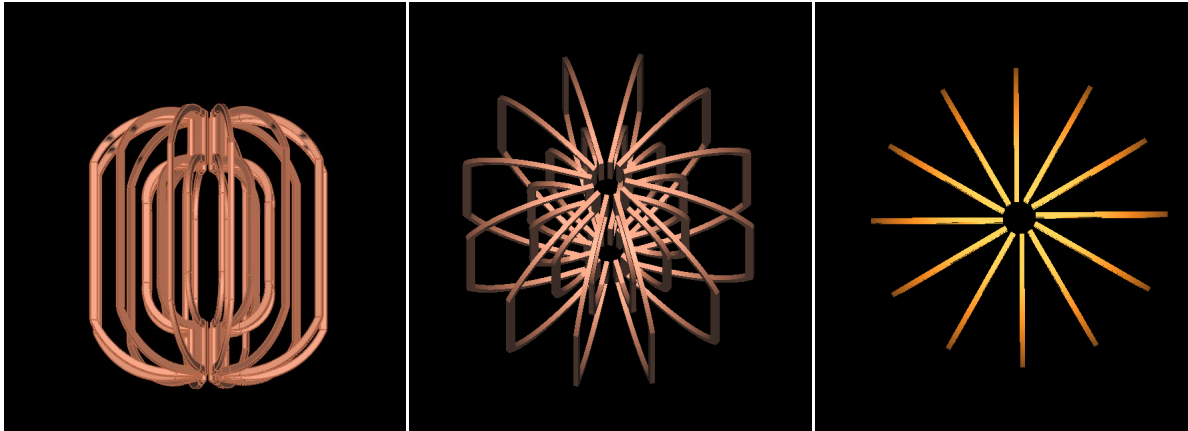


Figure 14. Three views of the prototype coil set for creating a toroidal magnetic field surrounding the habitat module of Fig. 13.

all magnetic field lines are closed, but in this case within the coil boundary). The Achilles heel of employing a simple circular or elongated cross section toroid is the lack of protection to GCR particles either directed or deflected into the polar regions of the habitat where there is little if any magnetic field perpendicular to the trajectory of the particles, thus allowing easy passage into the habitat. The first step was to consider the toroid that would most likely give the best shielding from all directions. The idea here is to shape the toroid to minimize this vulnerability (see Fig.14). By having the toroid shape be concave allowing the coils to wrap around the ends of the module provides for substantial

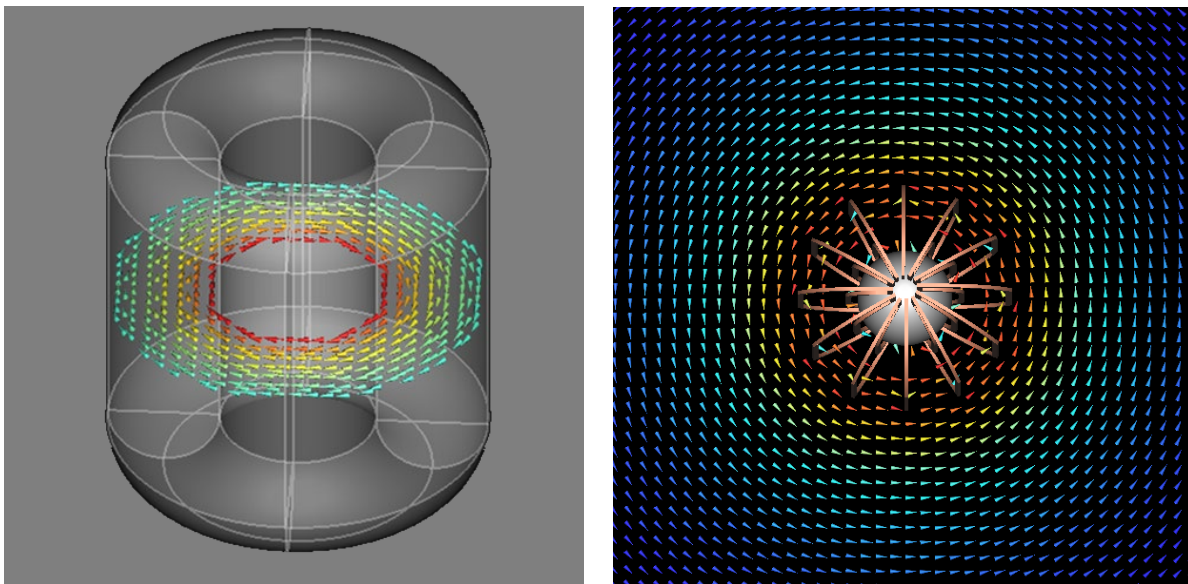


Figure 15. (Left) Magnetic field vector plot in midplane of the ESA toroid. (Right) Magnetic field vector plot in midplane of the hybrid “open” toroid. Field line are plotted for regions where the magnetic field magnitude is 5% of the peak magnetic field or larger.

shielding of GCR coming in from the ends of the module. The coil design was also constrained to a size that could fit into the fairing of the rocket similar to the one used to launch the SLS Derived Module. This would allow for the magnet and supporting casing structure to be fabricated on Earth for easy assembly in space, and thereby avoid issues involved with magnet inflation and deployment that had hampered previous magnetic shielding concepts.

In order to take advantage of an external field component as in the DTM, the idea was to construct the toroid from a set of discrete dipole coils that would be arranged around a circle in the toroidal direction such that the coil spacing on the outboard side of the toroid would be quite open, but a much closer spacing on the inboard spacecraft side of the toroid. A fully populated toroid with twelve coils as shown in Fig. 14. As can be seen in Fig. 14 that the shape of the conductors for the toroidal field reach down close to the axis at each end providing end protection. It is believed that the set of essentially 12 dipole field coils combined into an array will allow for a significant external field concentrated around each coil, as well as take advantage of the deflection of GCR at distance further away from the coils and spacecraft as in the DTM. This turned out to be doable and 12 dipole coils so arranged did indeed considerably increase the external magnetic field as can be seen in the magnetic field vector plots in the midplane of the toroidal coils shown in Fig. 15. It can also be seen that the field vanishes as desired inside the region to be occupied by the habitat. The more open nature of the toroid allows for the magnetic field to extend considerably outside the toroid as well as concentrates the currents into discrete segments so that the positive effects described in the discussion of the DTM and discrete current concentration (see Fig. 12) should be applicable here. The very open arrangement also minimizes the coil's exposure to the GCR. While the inner coils are much closer together, there should have been a significant reduction in incoming GCR by the strong toroidal fields inside the toroid by that point, and the high magnetic field near the inner windings is on the protective, outer side of the coils. The closer coil spacing is also important for keeping the local magnetic fields surrounding the coils from penetrating too far into the space habitat.

The difference in the magnetic fields from the original ESA toroid that employed a near continuous array of poloidal currents thereby keeping the toroidal magnetic field inside the torus, to the DTM hybrid scheme proffered here can be clearly seen in Fig. 15. The magnetic field is in fact even stronger than that found for the DTM as the scale and volume of the toroid is much larger for the SLS module in this case. As was mentioned, increasing the magnet volume is always advantageous as far as efficiency of shielding (Ω) is concerned. The DRA5 scale habitat here is much larger than that of the Columbus module assumed in the ESA shielding studies. (~ 100 vs. ~ 500 m³) significantly which also improves shielding efficiency. This is made clear in Fig. 16. This is an expanded view of the attenuation compared to that of Fig. 9 with the addition of the finite current element DTM and the Hybrid DTM. With the increased habitat size and coil volume, the shielding from the Hybrid can be shown to be quite effective in reducing the polar exposure to GCR and also very effective at shielding GCR from the "barrel" region as well. It would appear that the exposure of the coils to secondary emission from GCR impact would also be substantially improved as the external field protection is as good if not better than the DTM. Of course, the ability to provide complete protection as in the DTM would require additional coil structures at the polar ends.

Needless to say, there would still be no way to provide an artificial gravity or planetary braking system, but this hybrid coil set would at least be consistent with the current DRA5 plans for the space habitat, and would provide for a HTSC coil profile that could fit in the fairing of a large Aries class rocket, and then be readily assembled onto the habitat in LEO.

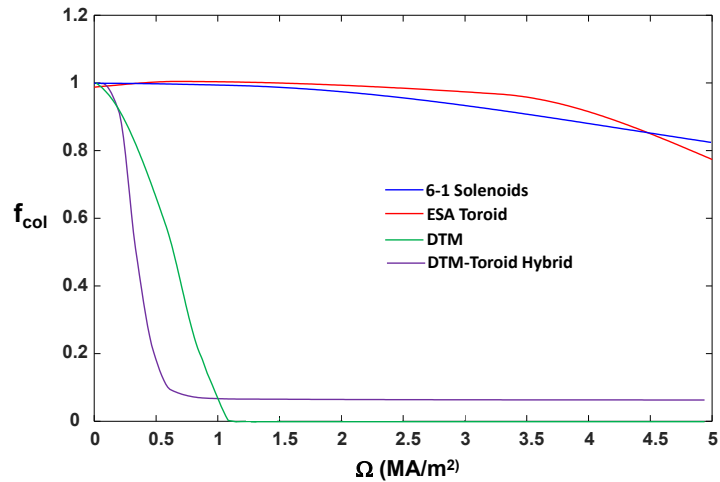


Figure 16. Fraction of 500 MeV protons reaching the habitat of the various concepts as a function of the efficiency parameter Ω .

VIII. Summary

An optimal magnetic shielding configuration for significantly reducing astronaut exposure to Galactic Cosmic Radiation (GCR) on long interplanetary missions has been realized, and is referred to as the Magnetospheric Dipolar

Torus (DTM). This configuration was shown to have the singular ability to deflect the vast majority of the GCR including High Z Energetic (HZE) ions. This external (to the spacecraft) dipolar field is created by an array of unidirectional toroidal High Temperature Superconductor (HTSC) windings mounted externally on the surface of the toroidally-shaped spacecraft habitat so that the spacecraft directly supports the magnetic hoop forces generated by the toroidal currents. The magnitude of the toroidal currents are arranged poloidally to flow so as to maintain the spacecraft shell as a constant flux boundary where the poloidal flux $\phi = 0$ inside the spacecraft keeping the habitat field-free. As the dipole magnetic field is perpendicular to the spacecraft habitat in all directions, the DTM provides a deflecting shield to all the incoming GCR which is nearly isotropic. In addition, the DTM shields the HTSC magnets as well thus eliminating the secondary particle irradiation hazard, which can dominate over the primary GCR for shields with closed magnetic topologies.

MSNW also developed 3-D relativistic particle code to evaluate magnetic shielding of GCR and employed a very accurate commercially available particle trajectory and magnetic field solver, Lorentz-3M, from Integrated Engineering to evaluate shielding effectiveness for the GCR spectrum encountered in space. The codes were employed to evaluate a wide range of magnetic topologies and shielding approaches including prior proposed magnetic shielding concepts. With DTM shielding it was found that both the structural and magnet mass as well as power requirements were significantly reduced. The DTM shielding effectiveness was calibrated in a large laboratory vacuum chamber experiment using a high energy beam as a surrogate for the GCR encountered in space.¹² It was discovered that by distributing the shielding currents in discrete cables, the local field concentration provided for a better shield for the magnets themselves, as well as reduced the penetration of GCR by a factor of about one half.

A DTM-Toroidal hybrid coil system was explored that could be used to shield the current NASA SLS Derived Laboratory Module. It was found the by using 12 dipole coils arranged in a toroidal array, and shaped to provide shielding in both the barrel and end regions of this habitat, a system for significantly reducing the GCR flux similar to the DTM could be achieved. It would also most likely provide a reduction in secondary irradiation as it also offers external magnetic shielding protection for both the habitat and magnetic coils.

Acknowledgments

The author would like to acknowledge and thank the NASA Innovative Advanced Concepts (NIAC) program for sponsoring this research.

References

- ¹Filippo Ambroglini, Roberto Battiston and William J. Burger, "Evaluation of Superconducting Magnet Shield Configurations for Long Duration Manned Space Missions", *Front. Oncol.*, 08 June 2016
- ²Jeffery C. Chancellor Graham B. I. Scott and Jeffrey P. Sutton, "Space Radiation: The Number One Risk to Astronaut Health, beyond Low Earth Orbit", *Life* 2014, 4, 491-510
- ³C. Zeitlin et al., "Measurements of Energetic Particle Radiation in Transit to Mars on the Mars Science Laboratory", *Science* 340, 1080 (2013)
- ⁴Shayne Westover et al, "Magnet Architectures and Active Radiation Shielding Study (MAARSS)", Final Report for NASA Innovative Advanced Concepts Phase II
- ⁵L.W. Townsend, "Overview of active methods for shielding spacecraft from energetic space radiation", *Phys Med.*, 2001;17 Suppl 1:84-5.
- ⁶Lawrence W. Townsend, Critical Analysis of Active Shielding Methods for Space Radiation Protection, *IEEAC paper #1094* (2004)
- ⁷Brun R, Bruyant F, Carminati F, Giani S, Maire M, McPherson A, et al. "Geant – "Detector Description and Simulator Tool" Geneva: CERN Program Library Long Write-up W5013, CERN (1994). p. 430.'
- ⁸Agostinelli S, Allison J, Amako K, Apostolakis J, Araujo H, Arce P, et al. "Geant4 – a simulation toolkit" *Nucl Instrum Methods A* (2003) 506:250. doi:10.1016/S0168-9002(03)01368-8
- ⁹Battiston R, Burger WJ, Calvelli V, Musenich R, Choutko V, Datskov VI, et al. "Superconductive Magnet for Radiation Shielding of Human Spacecraft. (2011)" Final Report ESTEC Contract N. 4200023087/10/NL/AF. Noordwijk.
- ¹⁰Pancotti, A., Slough, J., and Shimazu, A., "Mars Mission Trade Studies and Technology Development of a 36 MW Fusion Rocket", *Joint Conference of 30th International Symposium on Space Technology and Science, 34th International Electric Propulsion Conference*, July 2015
- ¹¹Bret G. Drake and Kevin D. Watts, "Human Exploration of Mars Design Reference Architecture 5.0 Addendum #2", NASA/SP-2009-566-ADD2
- ¹²John Slough, "Spacecraft -Scale Magnetospheric Protection from Galactic Cosmic Radiation", Final Report for NASA Innovative Advanced Concepts Phase II, September 2021.